DOE/NASA/2593-2
NASA TM-82591

High Temperature Alkali Corrosion in High Velocity Gases

Carl E. Lowell, Steven M. Sidik,
and Daniel L. Deadmore
National Aeronautics and Space Administration
Lewis Research Center

May 1981

Prepared for
U.S. DEPARTMENT OF ENERGY
Fossil Energy
Office of Coal Utilization

NOTICE

Changed
8-13-81

ERRATA

NASA Technical Memorandum 82591
DOE/NASA/2593-26

HIGH TEMPERATURE ALKALI CORROSION IN HIGH VELOCITY GASES

Carl E. Lowell, Steven M. Sidik, Daniel L. Deadmore
May 1981

Cover, title page, and last page: The DOE/NASA report number should be DOE/NASA/2593-28.

DOE/NASA/2593-28
NASA TM-82591

High Temperature Alkali Corrosion in High Velocity Gases

Carl E. Lowell, Steven M. Sidik,
and Daniel L. Deadmore
National Aeronautics and Space Administration
Lewis Research Center
Cleveland, Ohio 44135

May 1981

Work performed for
U.S. DEPARTMENT OF ENERGY
Fossil Energy
Office of Coal Utilization
Washington, D.C. 20545
Under Interagency Agreement EF-77-A-01-2593

HIGH TEMPERATURE ALKALI CORROSION IN HIGH VELOCITY GASES

by Carl E. Lowell, Steven M. Sidik,
and Daniel L. Deadmore

National Aeronautics and Space Administration
Lewis Research Center
Cleveland, Ohio 44135

ABSTRACT

The effects of potential impurities in coal-derived liquids such as Na, K, Mg, Ca, and Cl on the accelerated corrosion of IN-100, U-700, IN-792, and Mar-M509 were investigated using a Mach 0.3 burner rig for times to 1000 hours in 1-hour cycles. These impurities were injected in combination as aqueous solutions into the combustor of the burner rig. The experimental matrix utilized was designed statistically. The extent of corrosion was determined by metal recession. The metal recession data were fitted by linear regression to a polynomial expression which allows both interpolation and extrapolation of the data: As anticipated, corrosion increased rapidly with Na and K, and a marked maximum in the temperature response was noted for many conditions. In contrast, corrosion decreased somewhat as the Ca, Mg, and Cl contents increased. Extensive corrosion was observed at concentrations of Na and K as low as 0.1 ppm at long times.

E-838

INTRODUCTION

One of the major uncertainties in the use of coal-derived liquids to power gas turbines is the effect of residual impurities in such fuels on the life of the hot parts of the turbine. The effects of some of these impurities are known to be adverse. Much work has been done on the effects of impurities such as sodium (Na), potassium (K), and vanadium (V) (see refs. 1 to 5). Such impurities may react with the sulfur in the fuel during the combustion process forming highly corrosive deposits such as sodium and potassium sulfates, sodium vanadates, etc. These corrosive deposits lead to greatly accelerated attack on the hot airfoils of the turbine, resulting in unacceptably short lives. On the other hand, some impurities are known to act as corrosion inhibitors; for example, Ca and Mg (refs. 4 and 5) are often deliberately added to fuels to reduce corrosion. Finally, there are many impurities whose effects are not known and certainly the effects of the interaction of various impurities are largely unknown.

Two potential approaches to determining the effects of such impurities are fruitful. The first is to test many real fuels. By testing a broad spectrum of such fuels, the effects of the various impurities from the analyses of the fuels combusted can be inferred. The main advantage to this approach is that real fuels are burned and that one obtains data under conditions closely approaching those found in a real gas turbine. The main disadvantage of such tests is that the data obtained are relevant only to the fuels actually tested, and usually the range of impurities available is quite limited. Also, currently there are very few liquid coal-derived fuels that are available in quantities sufficient for such tests. The second approach involves the use of clean fuels doped with impurities of interest in a parametric fashion. The advantage of this approach is that such impurity combinations can be carefully controlled and varied in a systematic fash-

ion. This allows the prediction of attack due to any composition within the range of the impurities studied. The disadvantages to such tests are that they do not burn real fuels under real turbine conditions, and that many tests may be required.

The work described in this report is confined exclusively to the doping approach. The object of this effort is to evaluate the effects of time, temperature and impurity content on corrosion. An earlier report (ref. 6) described such tests. The impurities used in this earlier work were Na, K, Mg, Ca, and Cl, and other variables included in the tests were time, temperature, and fuel-to-air ratio. The temperature range covered in the earlier experiments was from 800° to 1100° C, and the time of the experiments ranged to 200 hours. The concentrations used in these experiments were centered around approximately 0.5 ppm, with variations from 5 to 0.05 ppm, approximately. The parametric additions of the impurities, as well as the other variables, were statistically designed to minimize the number of tests. While weight-change measurements were made, these data cannot be used to satisfactorily evaluate the extent of hot corrosion attack and metal recession measurements (τ) were used in their place. The types of deposits were evaluated by X-ray diffraction.

This work allowed the estimation of attack over a wide range of impurity concentrations at relatively short times; however, the extrapolation of such data to much lower concentrations and much longer times has limited validity. Therefore, the program was extended as described in the current paper to concentrations as low as 0.01 ppm, and to times as long as 1000 hours. Upon the completion of the experiments, most of the data were combined to be evaluated by multiple linear regression into one model. This model can then be used to estimate the effects of these impurities over a broad range of concentrations, temperatures, and times.

MATERIALS

The compositions of the alloys used in this program are listed in table I. The cobalt-base alloy Mar-M509 is a typical vane material which is generally considered to have good hot corrosion resistance due to its high chromium content. The three nickel-base turbine blade alloys cover a range of hot corrosion resistance: IN-792 has moderately good hot corrosion resistance, while U-700 has somewhat poorer hot corrosion resistance, and IN-100 has the least resistance to such attack. All of the alloys were cast by a commercial vendor into the shape shown in figure 1(a). All samples were grit blasted and cleaned with alcohol. Prior to test, each sample was measured along a diameter in the center of the expected hot zone (see fig. 1(a)) with a bench micrometer to a precision of ±2 micrometers and weighed to ±0.2 milligram.

PROCEDURE

A burner rig typical of the four used for these tests is shown in figure 1(b) and has been described in reference 7. Briefly, each rig is a nominal Mach 0.3 type fired with Jet A-1 fuel whose sulfur content was determined to be 0.035±0.014 weight percent over the duration of the tests which was approximately 2 years. The fuel-to-air mass ratio was varied from about 0.035 to 0.055. The dopants were injected into the combustion chamber as aqueous solutions. Eight samples were rotated rapidly in front of the exhaust nozzle and reached the desired temperature in a few minutes. After

each 1-hour exposure the burner pivoted away and a forced air cooling nozzle was directed onto the specimens for 3 minutes. Then this cycle was repeated.

At intervals, samples from each alloy were removed and new samples were put in their place. There were several replacement schedules followed during these tests, depending on the total duration of the test. Most of the schedules from the work described in reference 6 resulted in three samples from each alloy at the end of the test: one having been exposed for 40, one for 60, and one for 100 hours. In the later tests, however, where the impurity levels were at their lowest, the samples were scheduled such that at the conclusions of the test specimens were available with exposures of 100, 300, and 400 hours. In a few cases, samples were scheduled resulting in a final evaluation at 100, 400, 500, and 1000 hours.

Regardless of the time of exposure, after each sample was removed from the burner rig it was weighed, washed, and reweighed. Washing consisted of emersion of each sample blade in 300 cm^3 of water at 80° C, followed by a soft brushing in running water, an alcohol rinse and air drying. The samples were then sectioned along the plane shown in figure 1(a), which was the center of the hot zone, and where all temperature measurements were made during the run. The cut sections were mounted metallographically, polished and etched. Thickness measurements were made to determine the final thickness at maximum penetration and to calculate maximum metal loss τ, as shown in figure 2. While both the initial and final thicknesses were measured to a precision of ±2 micrometers, experience has shown (ref. 8) that the resultant change in thickness is only accurate to about ±20 micrometers at best, and is often as poor as ±200 micrometers, due to the irregularity of attack and other factors outlined in reference 7. At the conclusion of each test, and before washing, the samples of each alloy exposed for the longest time were scraped and the scrapings were submitted for powder diffraction to analyze the deposits. A few milligrams from each sample were obtained in this fashion and analyzed using a Guinier de Wolf camera. This type of focusing camera was necessary because of the complexity of the patterns of the deposits which resulted in many overlapping diffraction lines in the normal powder camera pattern.

RESULTS AND DISCUSSION

Model Choice and Fitting Procedures

In the preceding report (ref. 6) the data were fitted to:

$$\tau = C_1(Na)C_2(K)C_3(Mg)C_4(Ca)C_5(Cl)t^{\beta_1}\ 10^{\beta_2+\beta_3 T+\beta_4 T^2+E}$$

where each of the functions $C_i(X)$ is of the form

$$C_i(X) = \theta_{i1} + (1 - \theta_{i1})\ \exp(-X\theta_{i2}).$$

This particular model had fit the accumulated data about as well as the best fitting second order polynomial approximation, and had a much clearer interpretation. The added data gathered since then have been for considerably lower dopant concentrations and longer time as mentioned previously. Once the new data were included for fitting, making a total of 322 points per alloy, it became apparent that the simpler nonlinear model did not fit as well as the second order polynomial approximation. The model equation was

then modified to fit a polynomial approximating equation using multiple linear regression techniques. This procedure has the advantage that confidence intervals for estimated coefficients and predicted values are more easily determined (refs. 9 and 10).

Table II presents the raw data accumulated throughout the program; included are the X-ray diffraction results. The total range of dopant concentrations are shown schematically in figure 3. The first column of table II provides an identifier for the particular treatment combination, and the second column indicates the rig on which the test was run. The next five columns give the dopant concentrations in ppm, and the eighth column gives the test temperature in degrees C. These data consititute the test conditions. The corrosion products were subjected to X-ray diffraction analysis to identify compounds present. The five columns labeled phase strength provide such X-ray diffraction data as were available. That is, for each compound the strength of observed diffraction lines for any species indicated as being present was designated as weak, medium, strong, or dash for not observed. The next series of columns provide the time for which a specimen was exposed and the corresponding attack, τ. These data except for the 1000-hour values were fitted to a polynomial regression equation using the multiple linear regression analysis techniques as indicated above (refs. 9 and 10). The tentative models chosen were identified partly by using a basic second order polynomial in almost all the variables, that is, time, Na, K, Mg, Ca, Cl, and temperature. The interactions between time and chlorine and temperature were not included in the model because the experiment was somewhat unbalanced with respect to these factors. The 1000-hour data were not included because the combination of long time at very low dopant levels caused these tests to be at the extreme boundaries of the test conditions.

Examination of the data indicated that several three-factor interactions among some of the variables were likely. These were Na-Mg-Ca, K-Mg-Ca, Cl-Mg-Ca, temperature-Mg-Ca, Na-Cl-Mg, and K-Cl-Mg which were included in the model.

Table III presents all the terms of the polynomial considered and the results of the least squares regression. The final model was chosen by examining all the subset regressions using the Mallows Cp statistic as a criterion (ref. 10). Next the value of each estimated coefficient is given with its standard error in parenthesis. It must be pointed out that the scaling indicated in table III was required for each variable in order to achieve a reasonable degree of orthogonality among the terms of the model. Also included in table III are the coefficient of determination (R^2), the mean square error (s^2), the estimate of s, and the number of data points.

The nonlinear model of reference 6 was fitted to these data also, but the lack of its ability to accommodate various interactions caused its fit to be significantly poorer than the polynomial model.

The center point data analysis was presented previously (ref. 6). As mentioned there, the estimate, s^2, from those data should establish a criterion of comparison because all the variables are held as constant as possible so that the error represents the replication error and does not include any component due to a misspecified model equation. These estimates and estimates from other models are given in table IV.

As shown, the s^2 values using the nonlinear model and all data reported previously for IN-100, U-700, IN-792 are considerably larger than the center point values, while the Mar-M509 is only a little larger. Refitting a smaller data set to the same nonlinear model yields much smaller s^2 val-

ues for all alloys. In fact, only IN-100 remains much larger than the center point estimate. After including the low-dopant long-time data of this report, the nonlinear model turned out to be considerably poorer. The s^2 values listed in table IV for the polynomial models indicate that there is still some serious deficiency with respect to IN-100 (i.e., lack of fit with respect to the model), a less serious deficiency with respect to U-700 and IN-792, and that the s^2 for Mar-M509 is clearly not significantly different than the center point estimate. It is believed (ref. 11) that a large part of the discrepancy is due to the true shape of the τ against time curve that is shown in figure 4. This shape can be only approximated by the necessarily infrequent metal consumption measurements. Thus, using a simple term such as $\log_{10}$ (time) in the model is a serious oversimplification.

Implications of the Model

The models of table III are rather difficult to interpret in any direct examination of terms and coefficients. To facilitate understanding of the resulting equations, a series of parametric plots of attack are shown. Figures 5 to 8 illustrate the property that Na and K induce increased corrosion while Mg and Ca act as inhibitors. In figures 5 and 6, we hold K, Cl, temperature and time at constant values as listed, and plot predicted attack as a function of Na concentration for each of the four alloys. Indications of the reliability of the predictive regression equations are provided by representative two standard error limits on the estimated regression function. In figure 5, Mg and Ca are set at 0.1 ppm. In figure 6, we provide a similar plot of τ against Na, except that Mg and Ca are now at the 1 ppm level. Comparing these two plots shows a general reduction in attack for all alloys for the greater concentrations of Mg and Ca. The reduction is minimal for Mar-M509; it is substantial for IN-100 and U-700. Figures 7 and 8 provide similar plots to indicate the effects of Mg and Ca on K attack. Figure 7 shows the effect of K on attack with Mg and Ca held at 0.1 ppm, while for figure 8 with Mg and Ca set to 1 ppm. Figure 7 shows an increase in attack with K at the lower levels of Mg and Ca, but figure 8 shows little dependence of attack on K. The attack at high levels of K is greatly reduced at the higher levels of Mg and Ca. Figure 9 shows the effect of temperature on attack with all other variables held at their nominal center point values, that is, Na and K at 0.9 ppm, Ca and Mg at 0.47 ppm, Cl at 2.93 ppm, and time held at 100 hours. In general, for all the alloys, there is a maximum in the attack as a function of temperature or such a maximum can be inferred. At times the maximum is either at too low a temperature or too high a temperature to be seen over the range of the test conditions. It is, in general, considered (see ref. 1) to result from hot corrosion being confined to a temperature range in which the corrosive deposits are in their liquid phase. Therefore, at temperatures above the dew point or below the melting point, corrosion should be slight while in the intermediate temperature range, corrosion should be accelerated. However, the fact that the maxima differ with alloy indicates a pronounced alloy chemistry effect.

Figures 10 and 11 are used to illustrate the effects of Cl. In figure 10, Mg, Ca, temperature, and time are held constant with Na and K at 0.1 ppm, while figure 11 is for Na and K held at 1 ppm. These show that increasing Cl decreases attack for both conditions of Na and K. This probably results from the tendency for Cl to decrease the dew points of sodium and potassium sulfates.

One of the most significant interactions indicated in table III is that between temperature and Ca. This interaction is illustrated for each alloy in figures 12 to 15. In each of these figures, Na, K, Mg, Cl, and time are held constant. There are three curves of attack as a function of temperature for three levels of Ca. In figures 12 to 15, there is some indication that the level of Ca affects location of the maximum attack. Higher levels of Ca shift the maximum to higher temperature for the Ni-base alloys IN-100, U-700, and IN-792. However, for Mar-M509, the interaction is seen to be entirely inhibition at low levels of Ca, but accelerating at high Ca levels. As an indication of longer time predictability figures 16(a) and (b) plots the observed and predicted 400 hour data for IN-792 and Mar-M509 respectively. These plots indicate approximately ±2X agreement between calculated and predicted values. This agreement seems to hold for U-700, IN-792, and Mar-M509 1000-hour results from LT21 run, but not for the LT22 run. The results are:

	IN-100		U-700		IN-792		Mar-M509	
	LT21	LT22	LT21	LT22	LT21	LT22	LT21	LT22
Observed:	11 431	208	2184	217	1082	297	384	134
Predicted:	3126	1960	2041	1564	793	614	471	445

It should be noted that the LT21 run combines both a very long time and very low dopant concentrations. Likewise the LT22 run combines the most extreme time and lowest concentrations of all dopants.

Deposit Identification

As a result of the many test conditions on the four alloys over the broad range of concentrations in temperature, there is a plethora of X-ray diffraction data. These data are presented in table II. In general, the dopants tended to form the same types of deposits regardless of concentration or the combination with other elements. Mg in the combustion products tended to deposit as MgO. Calcium, on the other hand, reacted with sulfur in the fuel to form primarily $CaSO_4$. Both of these phases can be predicted using the chemical equilibrium computer program of Gordon and McBride (ref. 12). This program has been used successfully for such complex systems (refs. 13 and 14). As expected, Na and K also deposited as sulfates. In the case of Na, sodium sulfate was the primary phase; however, it was found in three separate crystallographic modifications (types I, III, and V). K, when present in appreciable quantities, was found as potassium sulfate and also combined with sodium sulfate to form a mixed sodium, potassium sulfate. As noted in the previous work (ref. 6), a phase determined to be Na, K, Ca, Mg sulfate, with the formula $Na_8K_2Ca(SO_4)_6$, was found for many of the conditions. In a few cases, a sodium calcium sulfate glauberite was found and a few weak lines which were never identifed were seen in a few of the patterns. The presence of these phases presented few surprises, as such sulfates formed during reactions have generally been found in these types of tests and usually led to accelerated corrosion (ref. 1). However, because the melting and dew points of several phases, (e.g., $Na_8K_2Ca(SO_4)_6$), are unknown, the temperature range of maximum corrosive attack can only be estimated.

CONCLUDING REMARKS

An attempt has been made to study the corrosive attack of turbine airfoil alloys as a function of Na, K, Ca, Mg, Cl, temperature, and time utilizing a statistically designed burner rig program. The attack model which was developed from these results seems to account for most of the important first order effects. The model is sufficiently inclusive to allow predictions for concentrations from 0.01 to nearly 10 ppm, and for times from 40 to over 500 hours, and a temperature range of 800° to 1100° C. Most of the first order effects, and a few of the interactions, can be accounted for. The major limitation of the data, and hence the model which is drawn from it, is the inherent inaccuracy of the thickness measurements upon which all of the conclusions are based. A secondary problem is the possibility of a lack of fit in the model. In order for a more precise rendering of attack models with a better definition of the interactions of these attacks to be determined, a more precise method for evaluating the extent of hot corrosion attack must be developed. In spite of these limitations, the level of predictive capability developed here should be sufficient for qualitative estimations of the degree of severity of many future synthetic fuels.

REFERENCES

1. Stringer, J. F., "Hot Corrosion in Gas Turbines," MCIC-72-08, Battelle Columbus Labs., Columbus, Ohio, June 1972.
2. Stringer, J. F., "High Temperature Corrosion of Aerospace Alloys," AGARD-AG-200, Advisory Group for Aerospace Research and Development, Paris, 1975.
3. Lunt, H. E., "Hot Corrosion in Gas Turbines," ASME Paper No. 77-WU/FU-3, Nov. 1977.
4. Lee, S. Y., Young, W. E., and Vermes, G., "Evaluation of Additives for Prevention of High Temperature Corrosion of Superalloys in Gas Turbines," ASME Paper No. 73-GT-1, Apr. 1973.
5. Zetlmeisl, M. J., May, W. R., and Annond, R. R., "Corrosion Inhibitor for Vanadium-Containing Fuels," U.S. Patent 3,926,577, Dec. 1975.
6. Lowell, C. E., Sidik, S. M., and Deadmore, D. L., "Effect of Sodium, Potassium, Magnesium, Calcium and Chlorine on the High Temperature Corrosion of IN-100, U-700, IN-792 and Mar-M509," ASME Paper 80-GT-150, March 1980.
7. Lowell, C. E. and Deadmore, D. L., "Effect of a Chromium-Containing Fuel Additive on Hot Corrosion," Corrosion Science, Vol. 18, 1978, pp. 747-763.
8. Lowell, C. E. and Probst, H. B., "Effects of Composition and Testing Conditions on Oxidation Behavior of Four Cast Commerical Nickel-Base Superalloys," NASA TN D-7705, 1974.
9. Draper, N. R. and Smith, H., Applied Regression Analysis, John Wiley and Sons, Inc., NY, NY, 1966.
10. Neter, J. and Wasserman, W., Applied Linear Statistical Models, 1974, Richard D. Irwin, Inc., Homewood, IL.
11. Deadmore, D. L. and Lowell, C. E., "Nondestructive Evaluation of the Kinetics of High Gas Velocity Hot Corrosion," in preparation.

12. Gordon, S. and McBride, B. J., "Computer Program for Calculation of Complex Chemical Equilibrium Compositions, Rocket Performance, Incident and Reflected Shocks, and Chapman-Jouget Detonations," NASA SP-273, 1971.
13. Material Response From Mach 0.3 Burner Rig Combusion of a Coal-Oil Mixture by G. J. Santoro, F. D. Calfo and F. J. Kohl. NASA TM-81686, December 1980.
14. Deposition and Material Response From Mach 0.3 Burner Rig Combustion of SRC-II Fuels by G. J. Santoro, F. J. Kohl, C. A. Stearns, G. C. Fryburg and J. R. Johnston. NASA TM-81634, October 1980.

TABLE I. - COMPOSITION OF ALLOYS

[All values are weight percent.]

Element	Mar-M509	IN-792	U-700	IN-100
Cr	23	12.7	14.2	10
Ni	10	Balance	Balance	Balance
Co	Balance	9.0	15.5	15
Al	-------	3.2	4.2	5.5
Ti	0.2	4.2	3.3	4.7
Mo	-------	2.0	4.4	3.0
W	7	3.9	-------	-------
Ta	3.5	3.9	-------	-------
Nb	-------	0.9	-------	-------
V	-------	-------	-------	1.0
Mn	-------	-------	<0.01	-------
Fe	-------	-------	0.1	-------
Si	-------	-------	<0.1	-------
Zr	0.5	0.1	<0.01	0.06
B	-------	0.02	0.02	0.014
C	0.6	0.2	0.06	0.18

TABLE II. - SUMMARY OF RUN CONDITIONS, XRD RESULTS, AND METAL RECESSION

ID	RIG	DOPANT(PPM) NA	K	MG	CA	CL	TEMP (C)	PHASE STRENGTH A	B	C	D	E	TIME (HR)	ATTACK(MICROMETERS) IN100	U700	IN792	MM509
CPO	1	0.90	0.90	0.45	0.45	3.21	950	W	-	M	M	S					
													40	317	294	142	154
													60	554	444	148	73
													80	420	737	161	103
													100	639	708	254	227
CPO	2	0.90	0.90	0.45	0.45	3.21	950	W	-	M	M	S					
													40	268	359	168	103
													60	328	641	202	125
													80	362	637	172	117
													100	433	757	257	113
CPO	3	0.90	0.90	0.45	0.45	3.21	950	W	-	M	M	S					
													40	105	113	108	87
													60	224	116	199	76
													80	413	571	141	91
													100	222	132	169	181
CPO	4	0.90	0.90	0.45	0.45	3.21	950	W	-	M	M	S					
													40	285	433	156	178
													60	359	669	170	98
													80	319	583	118	78
													100	363	594	209	213
BCEFG	1	1.20	1.20	1.00	1.00	5.90	1000	-	-	-	S	S					
													40	94	89	83	138
													60	126	176	98	105
													100	258	291	133	166
CDEF	2	0.40	2.00	1.00	1.00	5.90	900	-	-	-	S	S					
													40	77	54	27	44
													60	74	88	48	77
													100	67	69	62	130
ACG	3	1.20	1.20	0.20	0.20	3.39	1000	M	W	-	-	-					
													40	32	83	104	85
													60	121	135	63	84
													100	140	150	124	206
CDEG	4	0.40	2.00	1.00	0.20	4.49	1000	-	M	-	M	M					
													40	97	98	85	126
													60	128	99	91	94
													100	186	121	108	251
ADE	1	1.20	1.20	1.00	0.20	4.99	900	M	M	-	W	S					
													40	171	95	61	58
													60	913	162	189	209
													100	1310	239	201	225
ABCD	2	2.00	2.00	0.20	0.20	3.39	900	S	S	W	-	W					
													40	764	284	180	205
													60	1299	723	230	242
													100	2490	1305	691	317
BCE	3	1.20	1.20	1.00	0.20	4.49	900	M	W	-	-	S					
													40	339	39	103	124
													60	696	107	150	135
													100	1417	404	311	217
CP1	4	0.90	0.90	0.45	0.45	3.21	950	W	-	M	M	S					
													40	240	130	93	83
													60	270	138	93	95
													100	548	491	173	154

A=$NA_2\ SO_4$ B=$K_x\ NA_{2-x}\ SO_4$ C=$NA_8\ CA\ K_2(SO_4)_6$ D=$CA\ SO_4$ E=MGO

TABLE II. - Continued.

ID	RIG	DOPANT(PPM) NA	K	MG	CA	CL	TEMP (°C)	PHASE STRENGTH A	B	C	D	E	TIME (HR)	ATTACK(MICROMETERS) IN100	U700	IN792	MM509
CP2	1	0.90	0.90	0.45	0.45	3.21	950	W	-	M	M	S					
													40	376	278	92	39
													60	387	354	134	135
													100	838	1109	184	112
BDG	2	1.20	1.20	0.20	0.20	1.43	1000	S	W	-	W	-					
													40	527	661	380	189
													60	540	923	450	194
													100	1102	1527	739	402
ACF	3	1.20	1.20	0.20	1.00	4.80	900	S	-	-	M	M					
													40	356	68	75	36
													60	793	115	42	58
													100	1312	156	247	83
BDF	4	1.20	1.20	0.20	1.00	2.84	900	S	-	-	S	S					
													40	486	110	62	64
													60	791	88	39	72
													100	1384	148	210	162
FG	1	0.40	0.40	0.20	1.00	2.84	1000	-	-	-	S	S					
													40	98	120	93	126
													60	151	143	83	87
													100	203	236	157	93
CP3	2	0.90	0.90	0.45	0.45	3.21	950	W	-	M	M	S					
													40	226	242	123	98
													60	244	403	116	116
													100	373	749	254	143
ABEG	3	2.00	0.40	1.00	0.20	4.99	1000	M	-	-	-	S					
													40	133	129	128	121
													60	121	227	93	150
													100	132	217	199	169
ABEF	4	2.00	0.40	1.00	1.00	6.41	900	-	-	-	M	S					
													40	84	73	66	52
													60	437	55	58	44
													100	839	79	70	96
ABCDFG	1	2.00	2.00	0.20	1.00	4.80	1000	S	-	-	-	-					
													40	591	632	345	127
													60	1324	994	490	262
													100	1365	1495	1005	328
(1)	2	0.40	0.40	0.20	0.20	1.43	900	-	M	-	-	S					
													40	288	67	49	74
													60	461	63	69	99
													100	233	106	207	134
CP4	3	0.90	0.90	0.45	0.45	3.21	950	W	-	M	M	S					
													40	185	181	42	85
													60	156	87	96	117
													100	346	303	215	190
ADEFG	4	1.20	1.20	1.00	1.00	6.41	1000	-	-	-	S	S					
													40	144	146	108	94
													60	164	229	134	149
													100	280	292	181	163
BCF	1	1.20	1.20	0.20	1.00	3.57	900	-	W	S	S	S					
													40	412	136	66	98
													60	568	133	88	74
													100	1192	156	90	150

A=$NA_2\ SO_4$ B=$K_x\ NA_{2-x}\ SO_4$ C=$NA_8\ CA\ K_2(SO_4)_6$ D=$CA\ SO_4$ E=MGO

TABLE II. - Continued.

ID	RIG	DOPANT(PPM) NA	K	MG	CA	CL	TEMP (C)	PHASE STRENGTH A	B	C	D	E	TIME (HR)	ATTACK(MICROMETERS) IN100	U700	IN792	MM509
BCG	2	1.20	1.20	0.20	0.20	2.15	1000	M	W	-	-	-	40	990	551	307	113
													60	1788	944	282	184
													100	2040	1464	647	309
ABCDEG	3	2.00	2.00	1.00	0.20	5.72	1000	M	M	-	-	S	40	357	468	215	133
													60	641	606	277	137
													100	912	789	626	186
BDEFG	4	1.20	1.20	1.00	1.00	5.17	1000	-	-	-	S	S	40	167	194	97	36
													60	280	149	154	67
													100	439	498	193	282
CD	1	0.40	2.00	0.20	0.20	2.15	900	-	S	-	-	S	40	697	130	300	139
													60	983	217	336	215
													100	1661	431	541	365
ABFG	2	2.00	0.40	0.20	1.00	4.08	1000	-	-	S	-	-	40	328	265	112	146
													60	344	682	308	133
													100	538	709	494	184
CDFG	3	0.40	2.00	0.20	1.00	3.57	1000	-	-	-	S	-	40	124	132	104	150
													60	118	162	115	207
													100	174	207	136	245
ACE	4	1.20	1.20	1.00	0.20	5.72	900	M	W	-	-	S	40	76	65	116	88
													60	286	137	144	125
													100	1134	227	220	188
BDE	1	1.20	1.20	1.00	0.20	3.76	900	W	M	-	-	S	40	457	58	164	119
													60	875	190	172	167
													100	1634	576	197	242
ADF	2	1.20	1.20	0.20	1.00	4.08	900	-	-	S	S	S	40	368	54	64	63
													60	671	109	73	67
													100	1393	170	137	108
EG	3	0.40	0.40	1.00	0.20	3.76	1000	-	-	-	S	S	40	74	76	81	35
													60	58	93	96	9
													100	113	142	129	121
ADG	4	1.20	1.20	0.20	0.20	2.66	1000	M	M	-	-	W	40	96	73	92	98
													60	130	145	143	52
													100	208	203	252	234
AB	1	2.00	0.40	0.20	0.20	2.66	900	S	-	-	-	M	40	655	237	241	66
													60	1011	149	239	57
													100	1771	437	482	55
ABCDEF	2	2.00	2.00	1.00	1.00	7.13	900	-	-	S	S	S	40	295	72	41	46
													60	397	62	74	50
													100	1004	149	95	72

A=$NA_2\ SO_4$ B=$K_x\ NA_{2-x}\ SO_4$ C=$NA_8\ CA\ K_2(SO_4)_6$ D=$CA\ SO_4$ E=MGO

TABLE II. - Continued.

ID	RIG	DOPANT(PPM) NA	K	MG	CA	CL	TEMP (C)	PHASE STRENGTH A	B	C	D	E	TIME (HR)	ATTACK(MICROMETERS) IN100	U700	IN792	MM509
EF	3	0.40	0.40	1.00	1.00	5.17	900	-	-	-	S	S	40	47	57	29	36
													60	57	131	24	75
													100	59	81	15	39
ACEFG	4	1.20	1.20	1.00	1.00	7.13	1000	M	-	-	S	S	40	120	128	65	94
													60	109	160	111	117
													100	214	213	132	138
CPEND	1	0.90	0.90	0.45	0.45	3.21	950	W	-	M	M	S	40	297	150	86	90
													60	424	192	88	80
													100	653	909	227	59
													200	1009	2066	531	233
CPEND	2	0.90	0.90	0.45	0.45	3.21	950	W	-	M	M	S	40	175	97	80	109
													60	298	246	172	77
													100	745	751	224	139
													200	1023	1150	403	177
CPEND	3	0.90	0.90	0.45	0.45	3.21	950	W	-	M	M	S	40	73	95	73	46
													60	172	95	92	78
													100	363	362	148	130
													200	544	779	275	124
CPEND	4	0.90	0.90	0.45	0.45	3.21	950	W	-	M	M	S	40	204	84	83	42
													60	204	480	99	56
													100	321	777	153	130
													200	702	928	366	166
A+	4	5.40	0.90	0.45	0.45	10.15	950	S	-	-	-	M	40	1191	592	296	73
													60	1656	956	368	100
													100	2861	1474	709	129
F+	4	0.90	0.90	0.45	4.95	11.17	950	-	-	-	S	W	40	132	99	26	118
													60	85	113	95	95
													100	276	142	131	32
E+	3	0.90	0.90	4.95	0.45	16.33	950	-	-	-	M	S	40	78	103	68	39
													60	127	107	90	76
													100	133	124	111	41
CPSTAR1	3	0.90	0.90	0.45	0.45	3.21	950	W	-	M	M	S	40	86	68	83	31
													60	93	110	106	63
													100	230	105	128	140
B-	3	0.49	0.90	0.45	0.45	3.21	950	-	-	-	S	M	40	88	59	62	100
													60	96	108	50	120
													100	121	138	79	154
C+	4	0.90	5.40	0.45	0.45	7.29	950	-	S	-	-	S	40	272	361	138	76
													60	355	539	309	130
													100	686	652	448	234

A=NA_2SO_4 B=$K_x NA_{2-x} SO_4$ C=$NA_8 CA K_2(SO_4)_6$ D=$CA SO_4$ E=MGO

TABLE II. - Continued.

ID	RIG	DOPANT(PPM) NA	K	MG	CA	CL	TEMP (C)	PHASE STRENGTH A	B	C	D	E	TIME (HR)	ATTACK(MICROMETERS) IN100	U700	IN792	MM509
F-	3	0.90	0.90	0.45	0.04	2.48	950	S	-	-	-	-	40	177	95	47	125
													60	386	338	121	115
													100	478	551	130	233
G-	3	0.90	0.90	0.45	0.45	3.21	800	-	-	S	-	S	40	168	17	21	27
													60	272	23	32	46
													100	859	29	27	106
G+	4	0.90	0.90	0.45	0.45	3.21	1100	-	-	S	-	S	40	206	243	162	189
													60	270	257	183	172
													100	344	453	255	336
CPSTAR2	4	0.90	0.90	0.45	0.45	3.21	950	W	-	M	M	S	40	88	95	65	116
													60	215	198	95	95
													100	578	565	215	125
D+	3	0.90	5.40	0.45	0.45	3.21	950	-	S	-	-	S	40	1379	866	278	352
													60	1105	1105	383	351
													100	3522	2149	1010	682
E-	4	0.90	0.90	0.04	0.45	2.01	950	-	-	S	-	-	40	123	131	79	97
													60	513	583	213	99
													100	335	472	305	123
A-	3	0.49	0.90	0.45	0.45	2.58	950	-	-	-	S	M	40	116	85	66	66
													60	114	68	75	125
													100	164	73	110	162
C-	4	0.90	0.49	0.45	0.45	2.84	950	-	-	S	M	S	40	255	130	78	97
													60	227	140	82	108
													100	383	312	145	82
B+	4	5.40	0.90	0.45	0.45	3.21	950	S	-	-	-	M	40	1299	1529	304	103
													60	2309	2399	664	302
													100	3290	3950	981	420
D-	3	0.90	0.49	0.45	0.45	3.21	950	-	-	S	S	S	40	143	72	58	87
													60	146	74	89	113
													100	207	122	124	101
ADE-2	3	1.20	1.20	1.00	0.20	4.99	900	S	-	-	-	S	40	298	54	63	129
													60	641	105	167	171
													100	1397	329	200	227
ACE-2	4	1.20	1.20	1.00	0.20	5.72	900	-	M	M	-	S	40	195	125	135	120
													60	630	155	235	134
													100	1125	348	272	236
D	3	0.40	1.20	0.20	0.20	1.43	900	-	S	M	-	S	40	546	80	121	139
													60	916	101	164	142
													100	1577	299	410	263

A=$NA_2\ SO_4$ B=$K_x\ NA_{2-x}\ SO_4$ C=$NA_8\ CA\ K_2(SO_4)_6$ D=$CA\ SO_4$ E=MGO

TABLE II. - Continued.

ID	RIG	DOPANT(PPM) NA	K	MG	CA	CL	TEMP (°C)	PHASE STRENGTH A	B	C	D	E	TIME (HR)	ATTACK(MICROMETERS) IN100	U700	IN792	MM509
ACDF	4	1.20	2.00	0.20	1.00	4.80	900	-	-	S	-	S					
													40	252	132	73	45
													60	596	121	77	62
													100	1105	142	221	88
C	3	0.40	1.20	0.20	0.20	2.15	900	-	S	M	-	S					
													40	449	80	105	81
													60	840	93	235	166
													100	1414	291	293	257
AF	4	1.20	0.40	0.20	1.00	4.08	900	-	-	S	M	M					
													40	129	70	58	43
													60	393	78	46	21
													100	1223	105	30	91
BE	3	1.20	0.40	1.00	0.20	3.76	900	S	-	S	-	S					
													40	282	85	72	185
													60	530	50	135	168
													100	1545	109	241	219
ABCEF	4	2.00	1.20	1.00	1.00	7.13	900	-	-	S	W	S					
													40	88	53	54	66
													60	349	92	52	58
													100	950	84	87	99
ABDFG	3	2.00	1.20	0.20	1.00	4.08	1000	M	-	S	-	-					
													40	584	636	285	100
													60	920	943	334	132
													100	1177	1541	681	230
BCDG	4	1.20	2.00	0.20	0.20	2.15	1000	-	S	-	-	W					
													40	681	412	331	119
													60	803	562	344	185
													100	1251	963	526	301
CP(ELS)1	4	0.90	0.90	0.45	0.45	3.21	950	W	-	M	M	S					
													40	86	82	65	97
													60	248	144	52	120
													100	332	362	134	115
CP(ELS)2	3	0.90	0.90	0.45	0.45	3.21	950	W	-	M	M	S					
													40	141	101	77	91
													60	217	205	93	85
													100	304	230	114	191
EXPAND 1	3	0.58	1.23	1.26	0.95	0.46	900	-	W	-	-	M					
													40	496	82	59	73
													60	809	136	88	108
													100	1646	818	147	138
EXPAND 3	4	1.50	3.90	1.00	0.75	0.60	900	-	-	-	W	-					
													40	872	442	244	271
													60	1413	620	345	325
													100	2677	1831	617	476
EXPAND 5	3	1.90	0.50	1.05	0.79	0.48	900	-	S	-	-	M					
													40	541	116	42	142
													60	962	203	66	133
													100	1819	582	181	232
EXPAND 7	4	4.70	1.50	0.83	0.63	0.60	900	-	M	-	-	-					
													40	667	228	146	145
													60	1366	1077	337	218
													100	1948	1952	759	299

A=$NA_2\ SO_4$ B=$K_x\ NA_{2-x}\ SO_4$ C=$NA_8\ CA\ K_2(SO_4)_6$ D=$CA\ SO_4$ E=MGO

TABLE II. - Continued.

ID	RIG	DOPANT(PPM) NA	K	MG	CA	CL	TEMP (C)	PHASE STRENGTH A	B	C	D	E	TIME (HR)	ATTACK(MICROMETERS) IN100	U700	IN792	MM509
EXPAND 2	3	0.58	1.23	1.26	0.95	0.46	1000	-	-	-	-	S	40	120	94	96	77
													60	174	305	175	81
													100	246	679	202	140
EXPAND 4	4	1.50	3.90	1.00	0.75	0.60	1000	-	-	-	-	S	40	1523	721	415	309
													60	2123	1002	551	393
													100	3716	1655	924	600
EXPAND 6	3	1.90	0.50	1.05	0.79	0.48	1000	S	W	-	-	M	40	435	432	149	98
													60	822	585	317	201
													100	1022	933	525	200
EXPAND 8	4	4.70	1.50	0.83	0.63	0.60	1000	S	W	-	-	M	40	1738	1417	766	304
													60	2424	1743	780	426
													100	4154	3343	1386	693
LT01	3	0.50	0.50	0.20	0.20	1.00	900	-	-	-	-	-	100	1390	278	182	146
													300	5608	2442	1151	454
													400	6349	2972	1482	539
LT02	4	0.50	0.50	0.20	0.20	1.00	1000	S	-	-	-	-	100	175	189	110	134
													300	356	322	289	268
													400	455	443	455	460
LT03	3	0.10	0.50	0.20	0.10	0.10	900	-	-	-	-	-	100	700	231	163	195
													300	2830	1478	872	482
													400	4811	2194	926	450
LT04	4	0.22	0.22	0.14	0.14	0.32	1000	-	-	-	-	-	100	125	142	105	166
													300	305	220	147	312
													400	412	387	317	277
LT05	4	0.22	0.22	0.14	0.14	0.32	800	-	-	-	-	-	100	653	81	104	111
													300	2413	155	326	313
													400	3006	1362	463	355
LT06	3	0.10	0.10	0.20	0.20	0.10	900	-	-	-	M	-	100	374	83	96	108
													300	1943	319	142	178
													400	2928	791	506	281
LT07	3	0.50	0.10	0.10	0.10	1.00	900	-	-	-	-	-	100	471	86	49	148
													300	4920	197	431	392
													400	8476	2585	504	470
LT08	4	0.90	0.04	0.45	0.45	1.00	950	-	-	-	-	-	100	923	609	246	161
													300	2246	2257	584	306
													400	3319	2245	1020	302
LT09	3	0.10	0.10	0.20	0.10	1.00	900	-	-	-	S	M	100	155	94	126	127
													300	156	112	100	136
													400	169	151	57	125

A=$NA_2\ SO_4$ B=$K_x\ NA_{2-x}\ SO_4$ C=$NA_8\ CA\ K_2(SO_4)_6$ D=$CA\ SO_4$ E=MGO

TABLE II. - Continued.

ID	RIG	DOPANT(PPM) NA	K	MG	CA	CL	TEMP (C)	PHASE STRENGTH A	B	C	D	E	TIME (HR)	ATTACK(MICROMETERS) IN100	U700	IN792	MM509
LT10	4	0.22	0.22	0.14	0.14	0.32	900	-	-	-	-	-					
													100	725	115	98	134
													300	3129	1892	454	310
													400	4430	2369	1171	248
LT11	3	0.10	0.10	0.10	0.10	0.10	800	-	-	-	-	-					
													100	443	26	145	39
													300	1313	60	125	163
													400	1184	131	135	262
LT12	4	0.50	0.50	0.10	0.10	0.10	900	-	-	-	-	-					
													100	1970	472	253	426
													300	5729	2535	1461	619
													400	10382	3739	1567	720
LT13	3	0.10	0.10	0.10	0.10	0.10	900	-	-	-	-	-					
													100	195	82	149	137
													300	482	89	245	239
													400	1512	243	263	263
LT14	4	0.10	0.50	0.10	0.20	0.10	900	-	-	-	-	-					
													100	1340	201	220	277
													300	3249	1677	711	320
													400	5681	2575	914	668
LT15	3	0.50	0.10	0.20	0.10	0.10	900	-	M	-	-	S					
													100	1595	129	145	154
													300	3833	568	994	271
													400	7975	1386	1092	402
LT16	4	0.04	0.90	0.45	0.45	1.00	950	-	-	-	-	S					
													100	127	105	136	231
													300	212	197	280	210
													400	307	261	252	315
LT17	3	0.10	0.50	0.10	0.10	1.00	900	-	-	-	-	-					
													100	359	131	59	123
													300	1609	169	137	193
													400	2334	607	189	302
LT18	4	0.10	0.10	0.10	0.10	0.10	1000	-	-	-	-	W					
													100	147	186	87	128
													300	272	272	224	181
													400	360	392	299	325
LT19	3	0.10	0.10	0.10	0.20	1.00	900	-	-	-	-	S					
													100	69	55	59	105
													300	99	120	126	118
													400	123	127	128	155
LT20	4	0.50	0.10	0.10	0.20	0.10	900	S	-	-	-	S					
													100	1546	48	55	165
													300	5522	855	592	301
													400	8409	1763	445	255

A=$NA_2\ SO_4$ B=$K_x\ NA_{2-x}\ SO_4$ C=$NA_8\ CA\ K_2(SO_4)_6$ D=$CA\ SO_4$ E=MGO

TABLE II. - Concluded.

ID	RIG	DOPANT(PPM) NA	K	MG	CA	CL	TEMP (C)	PHASE STRENGTH A	B	C	D	E	TIME (HR)	ATTACK(MICROMETERS) IN100	U700	IN792	MM509
LT21	4	0.10	0.10	0.10	0.10	0.10	900	-	-	-	-	-					
													100	84	30	31	57
													400	1640	511	314	299
													500	4018	985	422	341
													1000*	11431	2184	1082	384
LT22	3	0.04	0.04	0.01	0.01	0.01	900	-	-	-	-	-					
													100	63	43	39	58
													400	147	71	119	81
													500	108	110	110	105
													1000*	208	217	297	134
LT23	3	0.50	0.10	0.10	0.10	0.10	900	S	-	-	-	-					
													100	1065	66	110	179
													300	4374	218	463	267
													400	6611	1229	822	431
LT24	4	0.10	0.50	0.10	0.10	0.10	900	-	-	-	-	-					
													100	826	175	199	206
													300	3921	1791	486	546
													400	5940	2520	1060	605

*Lot included in the final regression analysis.

TABLE III. - ESTIMATED REGRESSION COEFFICIENTS FOR THE COMBINED MODEL

	Coefficient estimate (standard error)							
	IN-100 log (τ)		U-700 log (τ)		IN-792 log (τ)		Mar-M509 log (τ)	
Intercept	2.749		2.595		2.316		2.194	
t	1.014	(0.069)	1.142	(0.066)	0.901	(0.046)	.0.627	(0.041)
r_1	-0.053	(0.020)	-0.088	(0.020)	-0.056	(0.014)	0	
r_2	0		0.047	(0.019)	0		0	
r_1r_2	0.025	(0.016)	0.032	(0.018)	0		0	
Na	0.644	(0.046)	0.384	(0.046)	0.322	(0.032)	0.191	(0.027)
K	0.373	(0.042)	0.215	(0.022)	0.279	(0.028)	0.295	(0.025)
Mg	0.319	(0.089)	0		0		0.198	(0.042)
Ca	0.099	(0.076)	0		0.183	(0.045)	-0.061	(0.034)
Cl	-0.249	(0.024)	-0.092	(0.021)	-0.109	(0.015)	-0.126	(0.011)
T	-0.152	(0.017)	0.111	(0.017)	0.077	(0.011)	0.052	(0.009)
Na^2	-0.089	(0.123)	-0.040	(0.013)	-0.028	(0.008)	-0.023	(0.007)
NaK	-0.120	(0.044)	0		-0.062	(0.031)	-0.088	(0.025)
K^2	-0.049	(0.011)	0		-0.028	(0.088)	-0.027	(0.007)
NaMg	-0.284	(0.086)	-0.385	(0.091)	-0.297	(0.060)	0	
KMg	0		-0.281	(0.073)	-0.169	(0.053)	-0.107	(0.046)
Mg^2	-0.214	(0.040)	-0.281	(0.087)	-0.330	(0.057)	-0.445	(0.059)
NaCa	-0.203	(0.115)	-0.221	(0.092)	0		0	
KCa	-0.381	(0.094)	-0.187	(0.087)	-0.161	(0.064)	-0.089	(0.050)
MgCa	-1.321	(0.228)	-0.280	(0.190)	-0.713	(0.131)	-0.333	(0.085)
Ca^2	-0.718	(0.144)	-0.117	(0.035)	-0.282	(0.073)	0	
NaCl	0		-0.046	(0.015)	-0.047	(0.010)	0	
KCl	0		-0.050	(0.011)	-0.037	(0.008)	-0.016	(0.005)
MgCl	0		0		0		0.123	(0.018)
CaCl	(0.361)	(0.074)	0		0.112	(0.036)	0	
Cl^2	0.030	(0.005)	0.035	(0.010)	0.042	(0.006)	0.011	(0.002)
NaT	0.051	(0.022)	0.057	(0.022)	0.047	(0.015)	0	
KT	0		0		-0.033	(0.017)	0	
MgT	0		0		0		-0.109	(0.027)
CaT	0.178	(0.052)	0.203	(0.058)	0.298	(0.035)	0.210	(0.029)
ClT	0		0.018	(0.010)	0		0	
T^2	-0.013	(0.009)	-0.058	(0.010)	-0.019	(0.007)	0	
NaMgCa	0		0		0		-0.363	(0.125)
KMgCa	0		0		0		0	
ClMgCa	-0.236	(0.112)	-0.144	(0.085)	-0.159	(0.078)	0	
TMgCa	0		-0.293	(0.128)	0		0	
NaClMg	0.097	(0.031)	0.071	(0.039)	0.128	(0.026)	0	
KClMg	0		0.057	(0.031)	0		0	
Nat	0.191	(0.080)	0		0.130	(0.055)	0.098	(0.049)
Kt	0		0		0		0.109	(0.053)
Mgt	0		-0.172	(0.139)	-0.249	(0.098)	0	
Cat	0		-0.286	(0.141)	0		-0.399	(0.093)
S	0.257		0.249		0.170		0.150	
R^2	0.769		0.760		0.819		0.759	
S^2	0.0661		0.0621		0.0290		0.0226	

The variables in the polynominal equation are defined as:

τ = attack (microns)
t = $\log_{10}$ (time (hrs.)/100)
r_1 = {-1 for rigs 1, 2; +1 for rigs 3, 4}
r_2 = {-1 for rigs 1, 3; +1 for rigs 2, 4}
Na = ppm Sodium -.9
K = ppm Potassium -.9
Mg = ppm Magnesium -.47
Ca = ppm Calcium -.47
Cl = ppm Chlorine -2.93
T = (Temperature (°C) -950)/50

Also given are the coefficient of determination (R^2) and the standard error of estimate (s).

Results Based on n = 322 data points.

Terms were deleted based upon examination of all possible subset regressions using the Mallows C_p criterion.

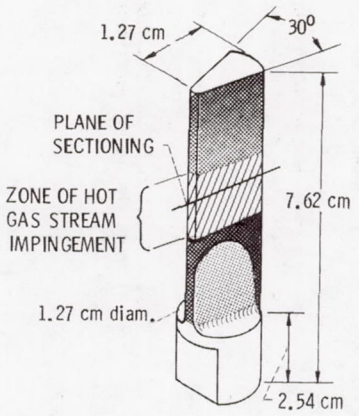

(a) TEST BAR.

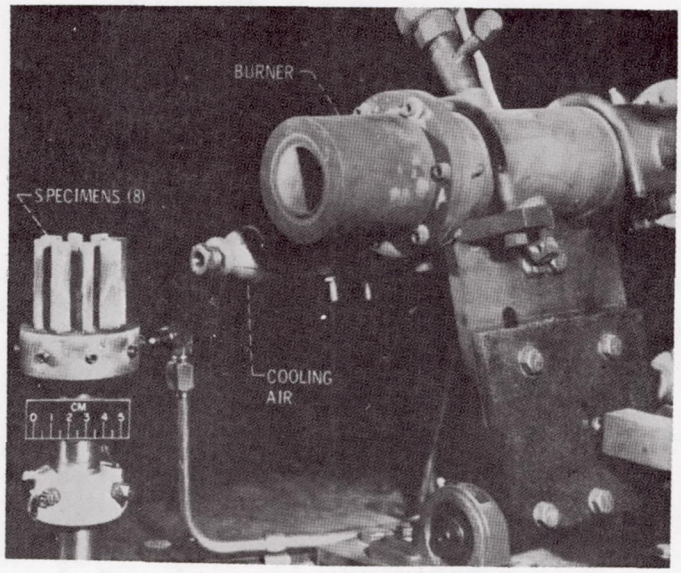

(b) BURNER RIG.

Fig. 1 Hot corrosion apparatus and test specimen.

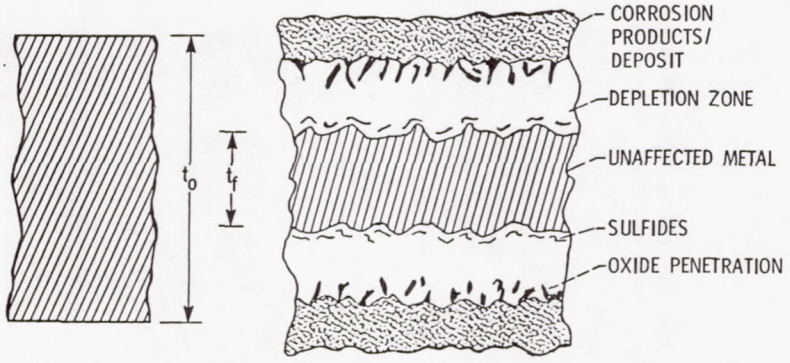

METAL RECESSION, τ, = $t_o - t_f$

Figure 2. - Measurement of extent of corrosion.

CS-80-1256

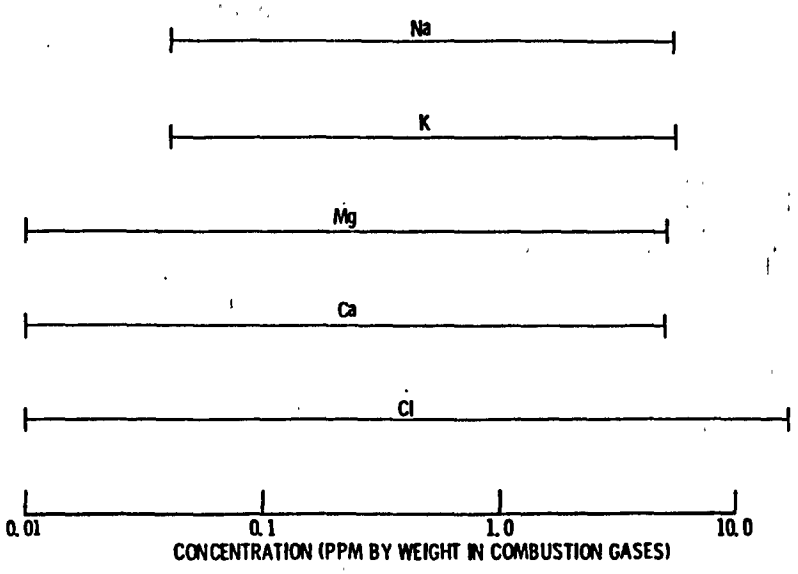

Figure 3. - Impurity range in doped fuel experiment.

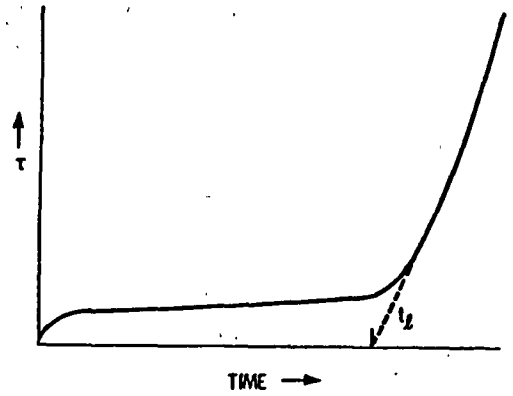

Figure 4. - Hot corrosion kinetics.

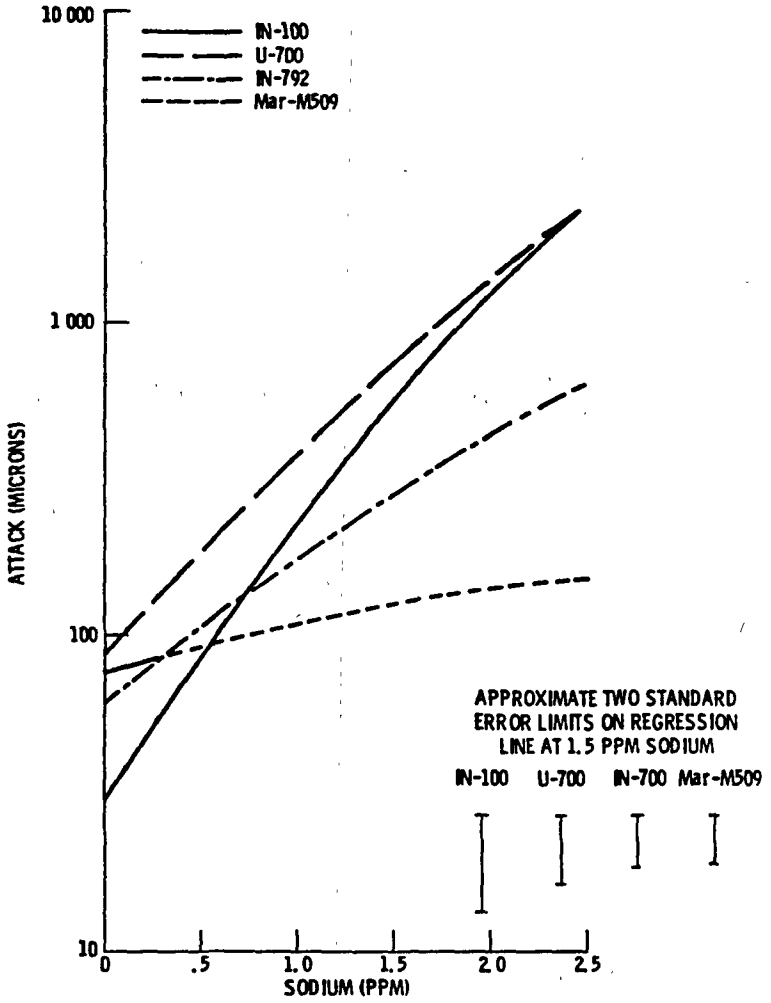

Figure 5. - Attack as a function of sodium with potassium (0.9 PPM), magnesium (0.10 PPM), calcium (0.10 PPM), chlorine (2.93 PPM), temperature (950° C) and time (100 hr) held constant.

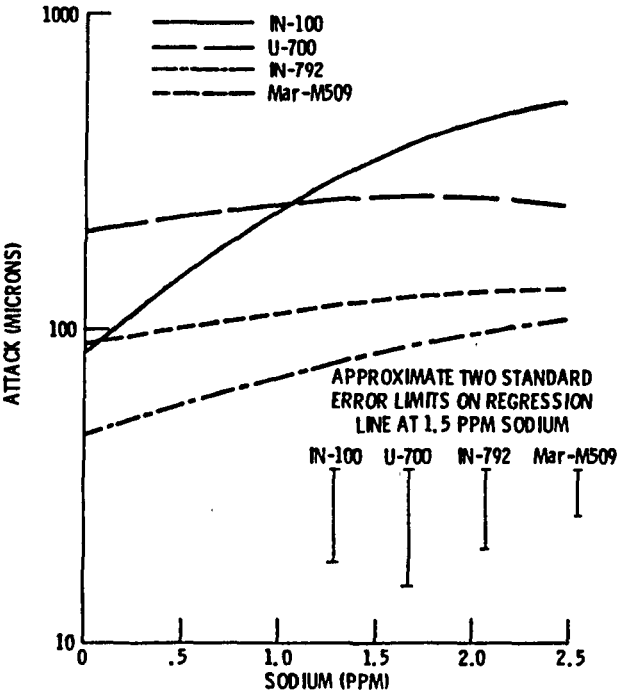

Figure 6. - Attack as a function of sodium with potassium (0.9 PPM), magnesium (1.0 PPM), calcium (1.0 PPM), chlorine (2.93 PPM), temperature (950° C), and time (100 hr) held constant.

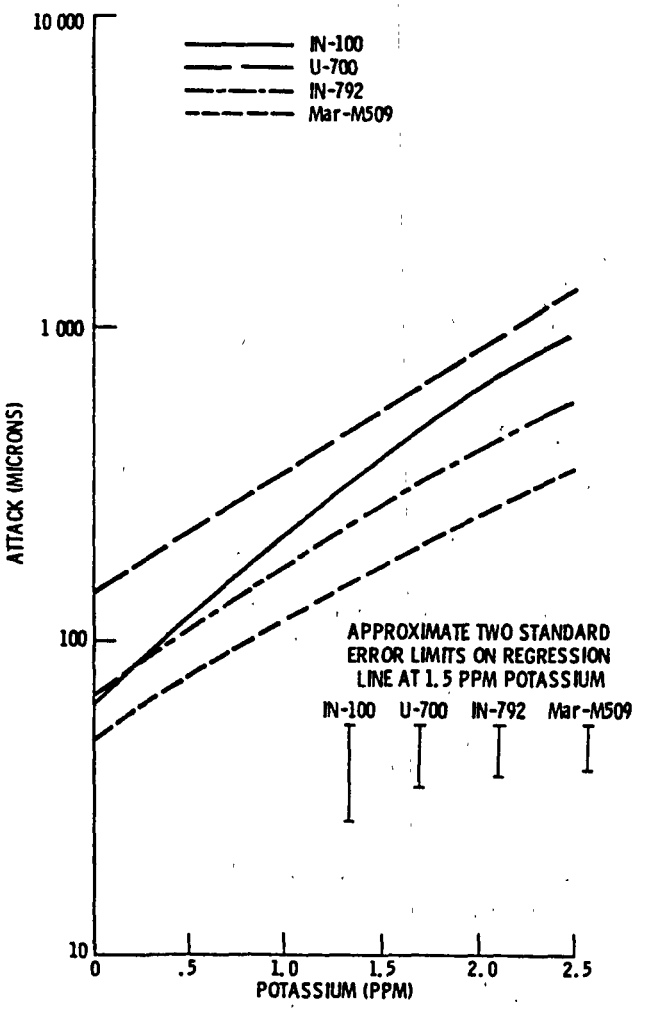

Figure 7. - Attack as a function of potassium with sodium (0.9 PPM), magnesium (0.1 PPM), calcium (0.1 PPM), chlorine (2.93 PPM), temperature (950° C), and time (100 hr) held constant.

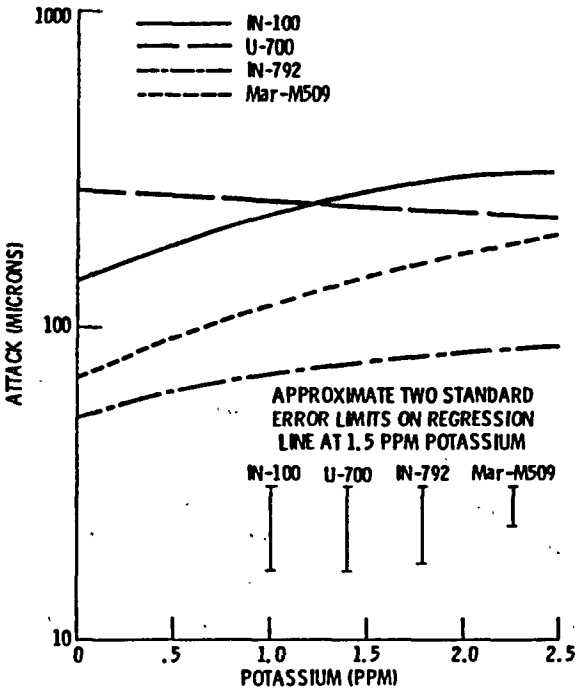

Figure 8. - Attack as a function of potassium with sodium (0.9 PPM), magnesium (1.0 PPM), calcium (1.0 PPM), chlorine (2.93 PPM), temperature (950° C), and time (100 hr) held constant.

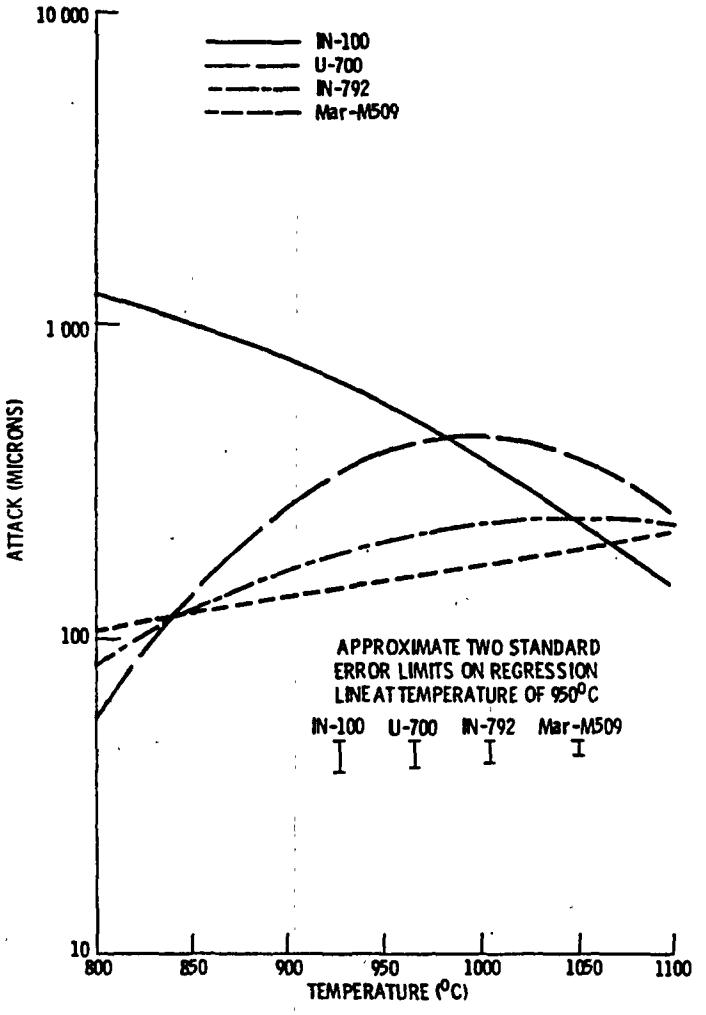

Figure 9. - Attack as a function of temperature with sodium (0.9 PPM), potassium (0.9 PPM), magnesium (0.47 PPM), calcium (0.47), chlorine (2.93 PPM), and time (100 hr) held constant.

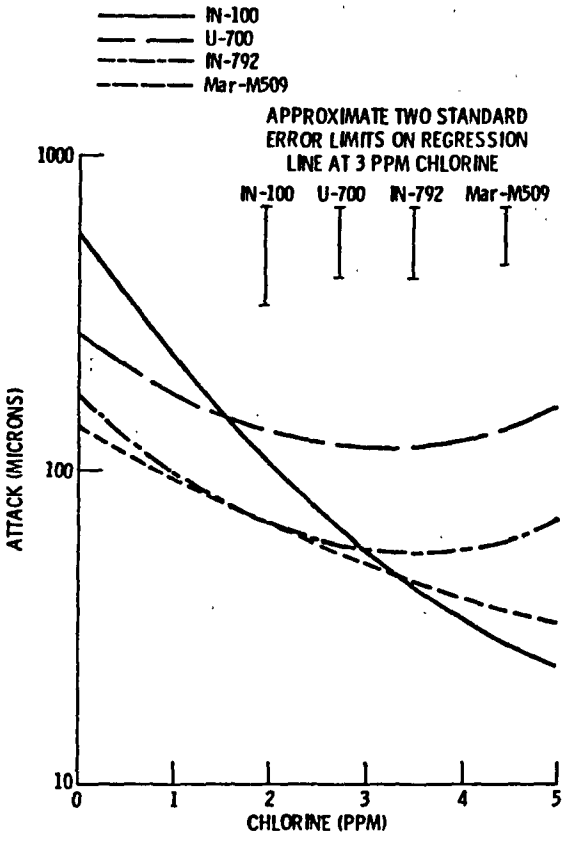

Figure 10. - Attack as a function of chlorine with sodium (0.1 PPM), potassium (0.1 PPM), magnesium (0.47 PPM), calcium (0.47 PPM), temperature (950° C), and time (100 hr) held constant.

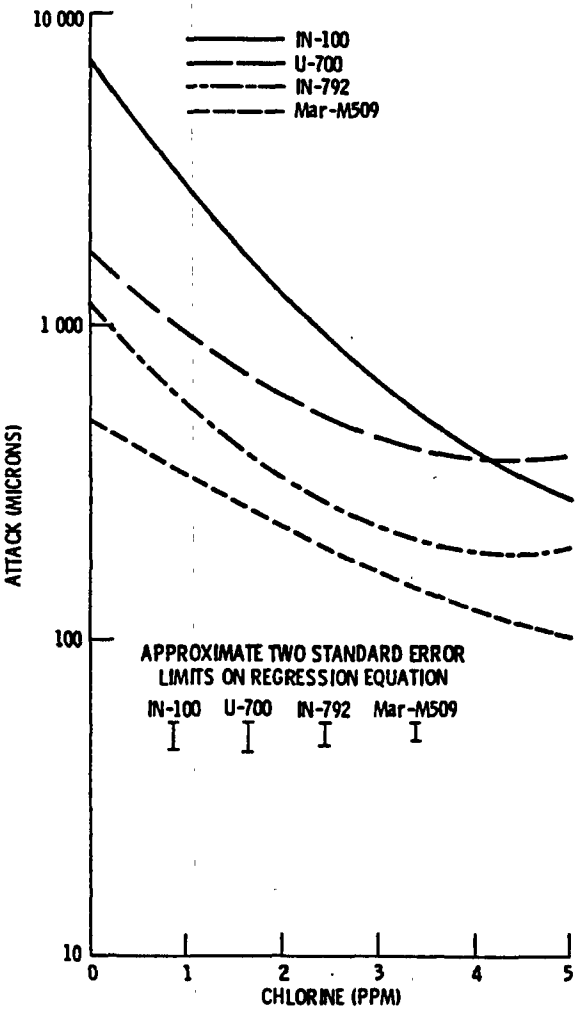

Figure 11. - Attack as a function of chlorine with sodium (1 PPM), potassium (1 PPM), magnesium (0.47 PPM), calcium (0.47 PPM), temperature (950°C), and time (100 hr) held constant.

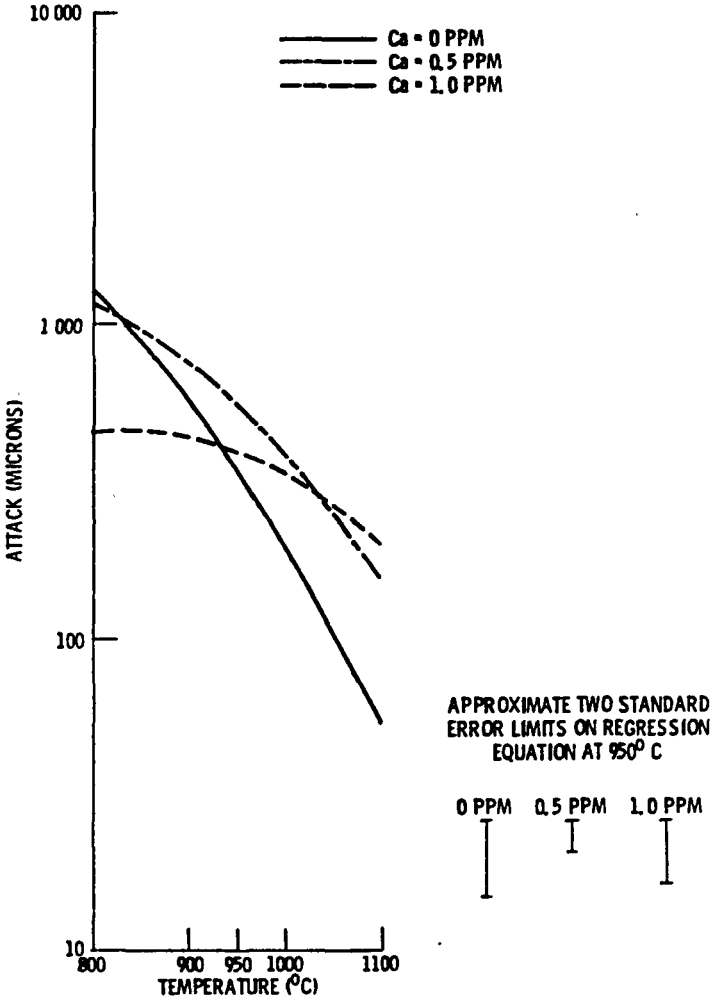

Figure 12. - Attack on IN-100 as a function of temperature at three different calcium concentrations with sodium (0.9 PPM), potassium (0.9 PPM), magnesium (0.47 PPM), chlorine (2.93 PPM), and time (100 hr) held constant.

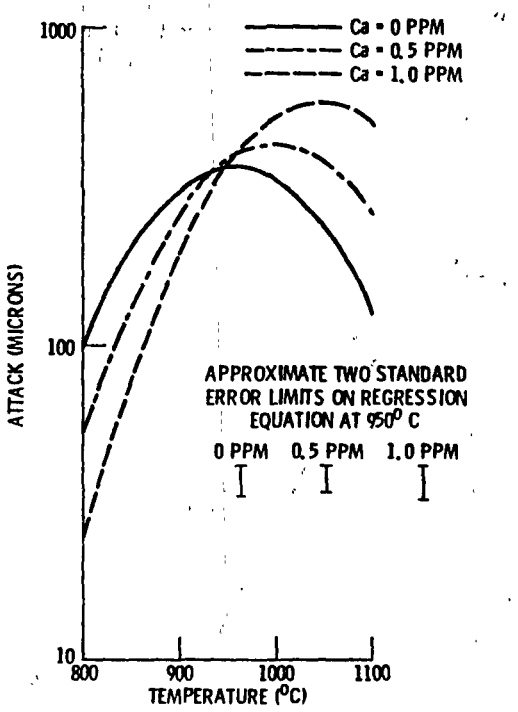

Figure 13. - Attack on U-700 as a function of temperature for the three different calcium concentrations with sodium (0.9 PPM), potassium (0.9 PPM), magnesium (0.47 PPM), chlorine (2.93 PPM), and time (100 hr) held constant.

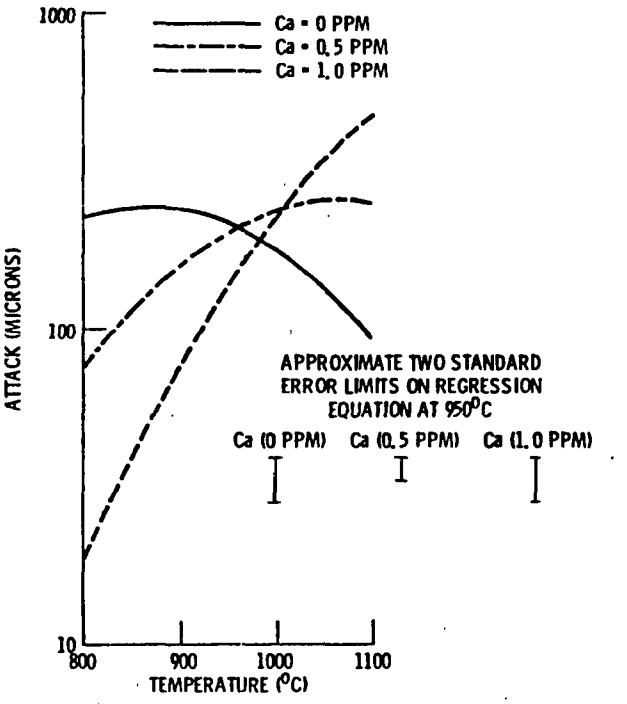

Figure 14. - Attack on IN-792 as a function of temperature for three different calcium concentrations with sodium (0.9 PPM), potassium (0.9 PPM), magnesium (0.47 PPM), chlorine (2.93 PPM), and time (100 hr) held constant.

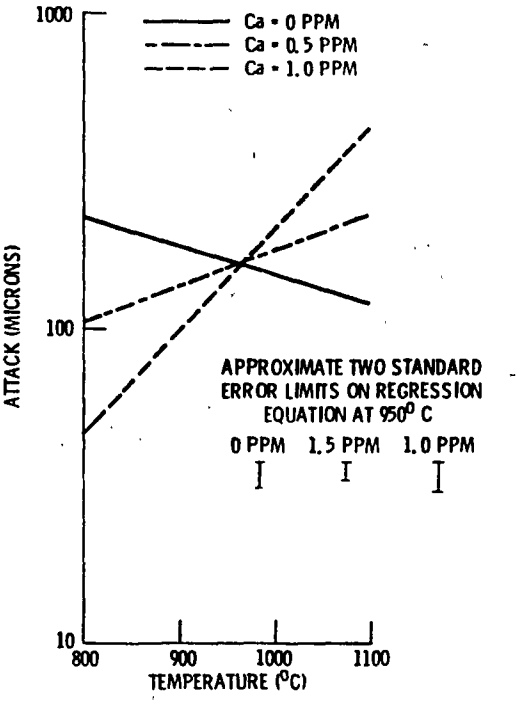

Figure 15. - Attack on Mar-M509 as a function of calcium with sodium (0.9 PPM), potassium (0.9 PPM), magnesium (0.47 PPM), chlorine (2.95 PPM), and time (100 hr) held constant.

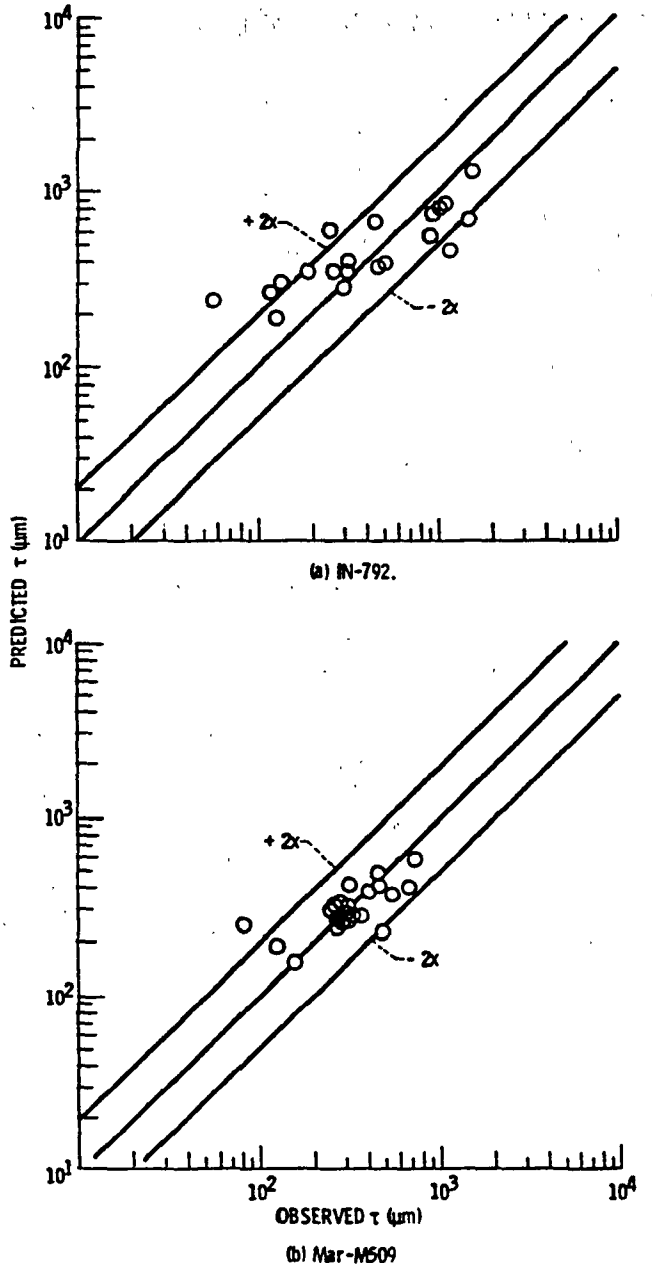

Figure 16. - A comparison of predicted and calculated metal recession values. 400 cycles of one hour at 900° C.

1. Report No. NASA TM-82591	2. Government Accession No.	3. Recipient's Catalog No.
4. Title and Subtitle HIGH TEMPERATURE ALKALI CORROSION IN HIGH VELOCITY GASES		5. Report Date May 1981 6. Performing Organization Code 778-11-06
7. Author(s) Carl E. Lowell, Steven M. Sidik, and Daniel L. Deadmore		8. Performing Organization Report No. E-838 10. Work Unit No.
9. Performing Organization Name and Address National Aeronautics and Space Administration Lewis Research Center Cleveland, Ohio 44135		11. Contract or Grant No.
12. Sponsoring Agency Name and Address U.S. Department of Energy Office of Coal Utilization Washington, D.C. 20545		13. Type of Report and Period Covered Technical Memorandum 14. Sponsoring Agency ~~Code~~ Report No. DOE/NASA/2593-29

15. Supplementary Notes

Final report. Prepared under Interagency Agreement EF-77-A-01-2593.

16. Abstract

The effects of potential impurities in coal-derived liquids such as Na, K, Mg, Ca and Cl on the accelerated corrosion of IN-100, U-700, IN-792 and Mar-M509 were investigated using a Mach 0.3 burner rig for times to 1000 hours in one-hour cycles. These impurities were injected in combination as aqueous solutions into the combustor of the burner rig. The experimental matrix utilized was designed statistically. The extent of corrosion was determined by metal recession. The metal recession data were fitted by linear regression to a polynomial expression which allows both interpolation and extrapolation of the data. As anticipated, corrosion increased rapidly with Na and K, and a marked maximum in the temperature response was noted for many conditions. In contrast, corrosion decreased somewhat as the Ca, Mg and Cl contents increased. Extensive corrosion was observed at concentrations of Na and K as low as 0.1 PPM at long times.

17. Key Words (Suggested by Author(s))

Corrosion
Alkali
Life prediction
High temperature
Superalloy
Deposition
Coal-derived fuel
Fuel impurities

18. Distribution Statement

Unclassified - unlimited
STAR Category 26
DOE Category UC-90h

19. Security Classif. (of this report)	20. Security Classif. (of this page)	21. No. of Pages	22. Price*
Unclassified	Unclassified		

* For sale by the National Technical Information Service, Springfield, Virginia 22161